Journal of Medicines Development Sciences, 2026, Volume 11, Issue 3
https://bbwpublisher.com/journal/JMDS
ISSN Online:2382-6371
ISSN Print:2382-6363

Recent Advances in Anti-aging for Sensitive Skin: Comprehensive Research on Spherical PDRN and Spherical Collagen Composite Systems—Innovations in Topical Baby Needles

Tiantian Wu[1]*, Tingting Zhang[2]*, Nan Zhang[2], Ying Zhang[1], Liming Wu[3], Lei Zhao[3], Yongjie Zhang[4]

[1]Shaanxi Bai'ao Regenerative Medicine Co., Ltd., Xi'an 710000, Shaanxi, China
[2]Xi'an Bohong Biotechnology Co., Ltd., Xi'an 710000, Shaanxi, China
[3]Xi'an Bohe Medical Technology Co., Ltd., Xi'an 710000, Shaanxi, China
[4]Guangdong Boxi Biotechnology Co., Ltd., Dongguan 523000, Guangdong, China

Author to whom correspondence should be addressed.

Copyright: © 2026 Author(s). This is an open-access article distributed under the terms of the Creative Commons Attribution License (CC BY 4.0), permitting distribution and reproduction in any medium, provided the original work is cited.

Abstract: *Objective:* At the forefront of anti-aging research for sensitive skin, we are developing a groundbreaking composite technology that integrates innovative spherical PDRN (Polydeoxyribonucleotide) with spherical collagen. This innovative system combines the remarkable efficacy of spherical PDRN in energy infusion, cellular repair, and deep anti-aging, with the significant advantages of spherical collagen in deep penetration, immediate replenishment of baby-like collagen, stimulation of collagen regeneration, and enhancement of skin firmness and elasticity. These two cutting-edge anti-aging technologies work synergistically to address the dual needs of skin "repair" and "anti-aging," providing cellular-level repair and direct collagen replenishment deep within the skin. This innovation offers a revolutionary skincare experience for those pursuing perfect skin, achieving the outstanding effects of a topical baby needle and rejuvenating the skin's youthful vitality. *Methods:* First, using confocal Raman spectroscopy, we precisely monitored the penetration behavior of spherical PDRN and spherical collagen, tracking the distribution of active ingredients at different skin depths in real-time to assess their transdermal capabilities. By comparing the penetration test results of unmodified PDRN and collagen with their spherical counterparts, we revealed the impact of the spherical shape on enhancing component penetration. Additionally, we conducted anti-degradation experiments on spherical PDRN to evaluate its stability within the biological system, which is crucial for maintaining the activity of the components during the transdermal process. Second, utilizing an ex vivo skin tissue model, we conducted in-depth research on the composite system of spherical PDRN and spherical collagen, focusing on eight types of collagen proteins: Collagen I, III, V, VI, VII, XVIII, XVII, and IV. This allowed us to accurately assess the efficacy of the composite system in promoting collagen proliferation, providing scientific evidence for the field of anti-aging in sensitive skin. Finally, we recruited volunteers with sensitive skin to participate in product testing, comparing the effects of the spherical PDRN and spherical collagen composite samples with those of salmon baby needle injections. Each participant's face was divided into two sides, with one side treated with the composite sample and the other side

receiving the injection, allowing for direct comparison of effects. To quantitatively evaluate the product's moisturizing, repairing, anti-wrinkle, and firming effects, we used the VISIA skin analysis system to compare and analyze the changes in skin indicators on both sides of the face. *Results:* ① Based on the penetration behavior studies using confocal Raman spectroscopy, the penetration test results of spherical PDRN and spherical collagen compared with unmodified PDRN and collagen are as follows: After 0. 5h, 1h, 2h, 4h, and 24h of penetration, spherical PDRN at a concentration of 0. 247mg/mL exhibited significant increases in the total integrated intensity under the peak at 1109cm^{-1}. After 0. 5h, 1h, 2h, 4h, and 24h of penetration, spherical collagen at a concentration of 0. 5mg/mL exhibited significant increases in the total integrated intensity under the peak at 1358cm^{-1}. After 0. 5h, 1h, 2h, 4h, and 24h of penetration, spherical peptides at a concentration of 0. 079mmol/L exhibited significant increases in the total integrated intensity under the peak at 1323cm^{-1}. ② Based on the Ex vivo skin tissue model, compared with the control group, the sample group showed significant increases in collagen content: Collagen I increased by 168. 89%, Collagen III by 190. 91%, Collagen IV by 146. 15%, Collagen V by 156. 41%, Collagen VI by 92. 16%, Collagen VII by 158. 82%, Collagen XVIII by 194. 59%, Collagen XVII by 190. 63%, elastin by 191. 43%, and collagen fiber content by 230. 10%.

Keywords: Spherical PDRN; Spherical collagen; Repair; Anti-aging; Sensitive skin; Eight types of collagen

Online publication: September 16, 2026

1. Experimental section

1.1. Main instruments and reagents

CO2 incubator (Thermo, 150I), upright microscope (Olympus, BX53), UVA irradiation device (Philips), laminar flow cabinet (Suzhou Antai, SW-CJ-1F), Cutometer MPA580 (CK, Germany), Corneometer CM825 (CK, Germany), Tewameter TM Hex (CK, Germany), microplate reader (BioTek, Epoch), Antera 3D (Delfin, Finland), TK-12D transdermal absorption diffusion apparatus (Shanghai Kaikai), Franz cell diffusion chamber (Shanghai Kaikai), 3D confocal Raman spectrometer (Witec Alpha, 500R), aesthetic (PDRN)product.

Ex vivo skin tissue culture medium (Guangdong Boxi Biotechnology), PBS (Solarbio), Vitamin C (VC, Sigma), Vitamin E (VE, Sigma), Elastin antibody (Abcam), Paraformaldehyde (Biosharp), Collagen I antibody (Proteintech), Collagen III antibody (Abcam), Collagen IV antibody (Abcam), Xylene (Sinopharm), Hematoxylin (Beyotime), Eosin (Beyotime), EpiGrowth culture medium (Guangdong Boxi Biotechnology), MTT (Sigma), Isopropanol (Sinopharm), Dexamethasone (China National Institute for the Control of Pharmaceutical and Biological Products), SLS (Sigma), IL-1α ELISA kit (Abcam), TNF-α ELISA kit (NOVUS), PGE2 ELISA kit (ENZO), PolyGanTec® spherical PDRN samples (Batch No. 231001), 3D epidermal skin model (EpiKutis® Batch No. ES241001), WY14643 (Sigma), FLG antibody (Abcam), LOR antibody (Abcam), Stirrer (EUROSTAR 60), PolyGanTec® spherical PDRN samples (Shaanxi Baihong Synthetic Biotechnology Co. , Ltd. , Batch No. 241002), PolyGanTec® spherical collagen samples (Shaanxi Baihong Synthetic Biotechnology Co. , Ltd. , Batch No. 231005), Butylene Glycol (OXEA), Glycerin (Hangzhou Zanu Oils & Fats Technology Co. , Ltd.), Acrylic (ester) / C10-30 alkyl acrylate crosslinked polymer (EVONIK), Preservatives.

1.2. In vitro testing methods

1.2.1. Transdermal absorption experiment

First, the ex vivo skin was fixed between the donor and receiver compartments of the Franz cell diffusion

chamber, with the stratum corneum facing the donor compartment and the dermal side facing the receiver compartment. 4. 0 mL of the receiver fluid was added to the receiver compartment. After tightening and fixing the ex vivo skin, 1 mL of receiver fluid (PBS) was added to the receiver compartment through a sampler, and the air was expelled to ensure close contact between the dermal side of the skin and the receiver fluid. For dosing: the sample was applied to the surface of the skin in the donor compartment, with an effective permeation area \(S \) of approximately 0. 785 cm^2. The sample was evenly spread from the center of the skin towards the periphery in a radial manner. To meet the statistical requirements for biological samples, each experimental group was set up with three replicates. For permeation: the magnetic stirrer was turned on to stir at a speed of 300 rpm, maintaining a constant temperature water bath at \((32 \pm 1) \)°C, and ensuring no air bubbles in the water bath jacket. Skin samples were collected at time points of 0. 5h, 1h, 2h, 4h, and 24h. The skin surface was washed five times, residual liquid on the surface was wiped dry with a cotton swab, and the skin was ring-cut with a blade. The samples were then frozen and sectioned for later use. Before detection, the confocal Raman spectrometer was calibrated using a silicon wafer. The quartz gold-coated slide with the frozen section was placed on the sample stage. Under the microscope, a site with no separation between the epidermis and dermis, no skin surface damage, no wrinkles, and clear structure was selected to measure its single spectrum. A point with prominent characteristic peaks and relatively low noise was chosen as the center to define the scanning area, and the Raman spectral dataset was obtained by scanning the sample.

1.2.2. Ex vivo skin model testing

The ex vivo skin model was placed into the culture inserts of a 6-well plate, with 3. 7 mL of culture medium added to each well. The models were then cultured in an incubator at 37°C with 5% CO_2, with the medium being changed daily. Irradiation and dosing: After 2 days of culture, the models were subjected to irradiation and dosing according to the test groups and corresponding treatment conditions. The irradiation doses were UVA (30 J/cm^2) and UVB (50 mJ/cm^2), with irradiation being performed for 4 consecutive days. After each irradiation, the culture medium was refreshed, and the dosing treatment was carried out. The test samples were applied topically. After 4 days of continuous irradiation, the ex vivo skin tissues were cultured for an additional 3 days without irradiation, but with continued sample application. Collagen fiber detection: Models designated for detection were fixed with 4% paraformaldehyde for 24 hours, followed by Masson's trichrome staining. The samples were then observed and photographed under a microscope, with images being captured and analyzed. Immunofluorescence detection: Models designated for detection were fixed with 4% paraformaldehyde for 24 hours, followed by immunofluorescence detection. The samples were then observed and photographed under a microscope, with images being captured and analyzed. Immunohistochemical detection: Models designated for detection were fixed with 4% paraformaldehyde for 24 hours, followed by immunohistochemical detection. The samples were then observed and photographed under a microscope, with images being captured and analyzed. Enhancement rate calculation: Enhancement rate (%) = ((Sample group - Negative control group) / Negative control) × 100%.

1.3. Statistical Analysis

In the transdermal absorption experiment, the Witec data analysis software was employed to obtain clearer spectra through methods such as spectral range selection, cosmic ray removal, polynomial fitting for baseline

correction, and smoothing of spectra using the Savitzky-Golay method. The Raman spectral dataset was analyzed using univariate analysis to extract the compositional information of the experimental samples. The Witec data analysis software completed univariate imaging, i. e. Raman spectral imaging. Pseudo-color image reconstruction could be performed based on the integrated intensity of characteristic peaks of a substance in the scanned spectra, with the intensity of the characteristic peaks being correlated to the brightness of colors in the Raman images. The Origin software was used to analyze the single-spectrum dataset, to plot the Raman spectra of multiple points across the full skin layer and the reconstructed Raman pseudo-color images after large-area scanning, as well as to conduct semi-quantitative analysis of the characteristic peaks of substances. GraphPad Prism was used for graphing, with results expressed as Mean ± SD. Comparisons between groups were statistically analyzed using the t-test method. All statistical analyses were two-tailed. A P-value of less than 0. 05 was considered to indicate a significant difference, while a P-value of less than 0. 01 was considered to indicate a highly significant difference.

The data were analyzed using SPSS 28. 0. The data were subjected to normality testing. If the test data followed a normal distribution, paired t-tests were used for statistical analysis. If the test data did not follow a normal distribution, the Wilcoxon signed-rank test (a type of rank-sum test) was used for statistical analysis. The significance level for the statistical methods was set at ($p < 0. 05$).

2. Test results

2.1. Results of the transdermal absorption experiment

As shown in **Table 1**, the results of the confocal Raman spectroscopy detection indicate that after 0. 5h, 1h, 2h, 4h, and 24h of penetration, the sample PDRN at a concentration of 0. 247mg/mL exhibited significant increases in the total integrated intensity under the peak at 1109cm^{-1}. After 0. 5h, 1h, 2h, 4h, and 24h of penetration, the sample PolyGanTec® spherical PDRN at a concentration of 0. 247mg/mL also exhibited significant increases in the total integrated intensity under the peak at 1109cm^{-1}. Compared with the PDRN-0. 247mg/mL group, the sample PolyGanTec® spherical PDRN-0. 247mg/mL showed significantly higher total integrated intensity under the peak at 1109cm^{-1} after acting on the skin for 0. 5h, 1h, 2h, 4h, and 24h. This indicates that the penetration performance of the sample PolyGanTec® spherical PDRN is superior to that of PDRN.

Table 1. Detection results of confocal Raman spectroscopy

Group	Time Point	Total Integrated Intensity(a.u.)	SD	*P*-value (vsPDRN-0.247mg/mL)	Enhancement Rate (vsPDRN-0.247mg/mL)
Blank Control	0h	0. 00	0. 00	/	/
PDRN-0. 247mg/mL	0. 5h	39. 37	2. 99	/	/
PolyGanTec® Spherical PDRN 0. 247mg/mL		88. 90	2. 75	0. 000**	125. 81%
PDRN-0. 247mg/mL	1h	44. 40	2. 17	/	/
PolyGanTec® Spherical PDRN 0. 247mg/mL		121. 21	3. 58	0. 000**	173. 00%
PDRN-0. 247mg/mL	2h	67. 68	1. 91	/	/
PolyGanTec® Spherical PDRN 0. 247mg/mL		202. 62	0. 20	0. 000**	199. 38%

Group	Time Point	Total Integrated Intensity(a.u.)	SD	*P*-value (vsPDRN-0.247mg/mL)	Enhancement Rate (vsPDRN-0.247mg/mL)
PDRN-0. 247mg/mL	4h	96. 17	5. 55	/	/
PolyGanTec® Spherical PDRN 0. 247mg/mL		283. 79	1. 24	0. 000**	195. 09%
PDRN-0. 247mg/mL	24h	114. 91	0. 43	/	/
PolyGanTec® Spherical PDRN 0. 247mg/mL		351. 94	1. 01	0. 000**	206. 27%

As shown in **Table 2**, the results of the confocal Raman spectroscopy detection indicate that after 0. 5h, 1h, 2h, 4h, and 24h of penetration, the sample collagen at a concentration of 0. 5mg/mL exhibited significant increases in the total integrated intensity under the peak at 1358cm^{-1}. After 0. 5h, 1h, 2h, 4h, and 24h of penetration, the sample PolyGanTec® spherical collagen at a concentration of 0. 5mg/mL also exhibited significant increases in the total integrated intensity under the peak at 1358cm^{-1}. Compared with the collagen-0. 5mg/mL group, the sample PolyGanTec® spherical collagen-0. 5mg/mL showed significantly higher total integrated intensity under the peak at 1358cm^{-1} after acting on the skin for 0. 5h, 1h, 2h, 4h, and 24h. This indicates that the penetration performance of the sample PolyGanTec® spherical collagen is superior to that of collagen.

Table 2. Detection results of confocal Raman spectroscopy

Group	Time Point	Total Integrated Intensity(a.u.)	SD	P-value (vsPDRN-0.247mg/mL)	Enhancement Rate (vsPDRN-0.247mg/mL)
Blank Control	0h	0. 00	0. 00	/	/
Collagen -0. 5mg/mL	0. 5h	66. 20	2. 25	/	/
PolyGanTec® Spherical Collagen -0. 5mg/mL		154. 64	0. 48	0. 000**	133. 60%
Collagen -0. 5mg/mL	1h	131. 13	6. 43	/	/
PolyGanTec® Spherical Collagen -0. 5mg/mL		376. 41	1. 35	0. 000**	187. 05%
Collagen -0. 5mg/mL	2h	173. 36	2. 59	/	/
PolyGanTec® Spherical Collagen -0. 5mg/mL		505. 11	3. 17	0. 000**	191. 36%
Collagen -0. 5mg/mL	4h	172. 89	3. 14	/	/
PolyGanTec® Spherical Collagen -0. 5mg/mL		561. 57	1. 29	0. 000**	124. 81%
Collagen -0. 5mg/mL	24h	211. 50	1. 36	/	/
PolyGanTec® Spherical Collagen -0. 5mg/mL		730. 51	1. 64	0. 000**	245. 39%

2.2. Ex vivo skin model testing

Using ex vivo skin tissue, the morphology of the tissue was examined in vitro. In this test, ex vivo skin tissue was subjected to combined irradiation with UVA and UVB. By detecting the changes in the content of Collagen IV, Collagen VI, Collagen XVI, and Elastin, the firming efficacy of the tested samples was evaluated. Meanwhile, by detecting the changes in the content of Collagen I, Collagen III, Collagen V, Collagen VI, Collagen XVIII, and collagen fibers, the anti-wrinkle efficacy of the tested samples was assessed.

2.2.1. Detection results of Type I collagen content

As shown in **Table 3**, compared with the BC group, the content of Collagen I in the NC group significantly decreased, indicating that the test stimulation conditions were effective. Compared with the NC group, the content of Collagen I in the PC group significantly increased, indicating that the positive control in this test was effective. Compared with the NC group, the content of Collagen I in the sample group significantly increased, with an enhancement rate of 168. 89%.

Table 3. Summary of detection results for type I collagen content

Sample Name	Relative Average IOD (Integrated Optical Density)	SD	*P*-value	Enhancement Rate(*vs*NC)
BC(Blank)	1. 00	0. 17	/	/
NC(Negative)	0. 45	0. 04	0. 005##	/
PC(VC+VE)	0. 95	0. 12	0. 002**	/
Test Sample	1. 21	0. 10	0. 000*	168. 89%

Notes: When statistical analysis was performed using the t-test method, significance compared with the BC group is indicated by #, with (P)-value < 0. 05 represented as # and (P)-value < 0. 01 represented as ##; significance compared with the NC group is indicated by *, with (P)-value < 0. 05 represented as * and (P)-value < 0. 01 represented as **

2.2.2. Detection results of type III collagen content

As shown in **Table 4**, compared with the BC group, the content of Collagen III in the NC group significantly decreased, indicating that the experimental stimulation conditions were effective. Compared with the NC group, the content of Collagen III in the PC group significantly increased, indicating that the positive control detection was effective. Compared with the NC group, the content of Collagen III in the sample group significantly increased, with an enhancement rate of 190. 91%.

Table 4. Summary of detection results for Type III collagen content

Sample Name	Relative Average IOD (Integrated Optical Density)	SD	*P*-value	Enhancement Rate(*vs*NC)
BC(Blank)	1. 00	0. 14	/	/
NC(Negative)	0. 33	0. 04	0. 001##	/
PC(VC+VE)	1. 08	0. 13	0. 001**	/
Test Sample	0. 96	0. 11	0. 001 *	190. 91%

Notes: When statistical analysis was performed using the t-test method, significance compared with the BC group is indicated by #, with (P)-value < 0. 05 represented as # and (P)-value < 0. 01 represented as ##; significance compared with the NC group is indicated by *, with (P)-value < 0. 05 represented as * and (P)-value < 0. 01 represented as **

2.3. Based on the epidermal model—testing the inhibition of inflammatory factors

2.3.1. Detection results of skin thickness

As shown in **Table 5**, compared with the BC group, the viable cell layer in the NC group was damaged, with vacuoles appearing, indicating that the test stimulation conditions were effective. Compared with the NC group, the viable cell layer in the PC1 group had a more compact cell arrangement, reduced vacuoles, and a significant improvement in cell damage, indicating that the positive control in this test was effective. Compared with the NC group, the sample group showed more compact cell arrangement in the viable cell layer, reduced vacuoles, and significant improvement in cell damage.

Table 5. Summary of detection results for epidermal thickness

Sample Name	Relative Average IOD (Integrated Optical Density)	SD	*P*-value	Enhancement Rate(*vs*NC)
BC(Blank)	125. 91	2. 78	/	/
NC(Negative)	84. 58	2. 23	0. 000##	/
PC(VC+VE)	93. 86	2. 48	0. 009**	/
Test Sample	97. 11	2. 73	0. 002 *	14. 81%

Notes: When statistical analysis was performed using the t-test method, significance compared with the BC group is indicated by #, with (P)-value < 0. 05 represented as # and (P)-value < 0. 01 represented as ##; significance compared with the NC group is indicated by *, with (P)-value < 0. 05 represented as * and (P)-value < 0. 01 represented as **

2.3.2. Results of soothing efficacy testing

2.3.2.1. Results of IL-1α inhibition rate testing

As shown in **Table 6**, compared with the BC group, the content of IL-1α in the NC group significantly increased, indicating that the test stimulation conditions were effective. Compared with the NC group, the content of IL-1α in the PC group significantly decreased, indicating that the positive control in this test was effective. Compared with the NC group, the content of IL-1α in the test sample significantly decreased, with an inhibition rate of 45. 12%.

Table 6. Inhibition rate of IL-1α

Sample Name	Average Concentration (pg/mL)	SD	*P*-value	Inhibition Rate(*vs*NC)
BC(black)	7. 62	0. 32	/	/
NC(Negative)	31. 58	0. 71	0. 000##	/
PC(Dexamethasone)	17. 10	0. 20	0. 000**	/
Test Sample	17. 33	0. 25	0. 000**	45. 12%

2.3.2.2. Results of in vivo efficacy testing

The images of some subjects are shown as follows:

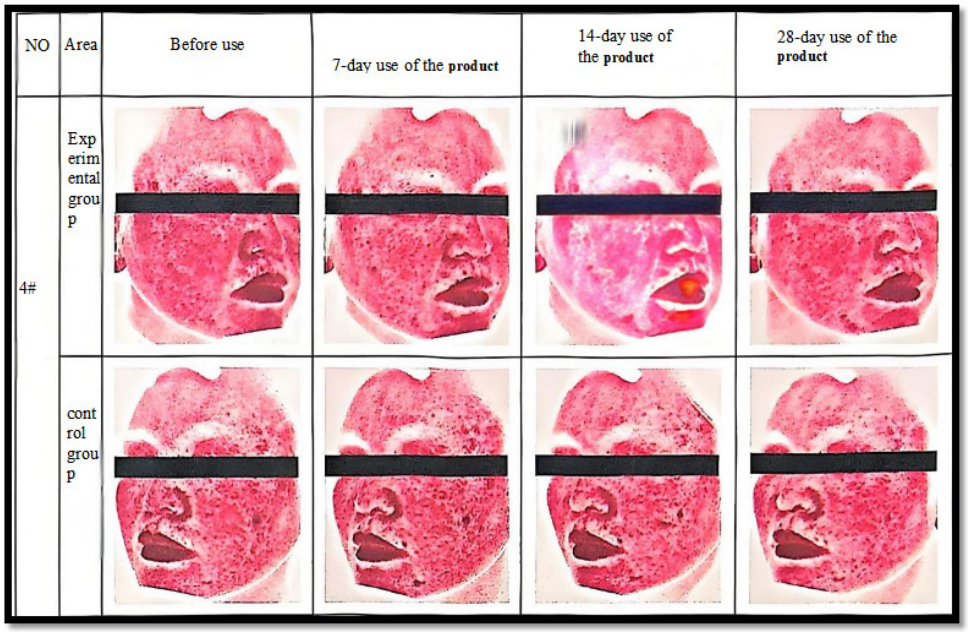




Figure 1. Comparative display of test images at different time points.

Based on the validation of the product used by the 10 subjects, the following conclusions were drawn: No adverse skin reactions were observed in either the test group or the control group within 7 days (7d), 14 days (14d), and 28 days (28d) of using the product. At 7d, the test group showed statistically significant results ($P < 0.05$), with a higher rate of change than the control group; at 14d, the test group showed statistically significant results ($P < 0.05$); at 28d, the test group showed statistically significant results ($P < 0.05$). At 7d, the rate of change in the test group was higher than that of the control group; at 14d, the test group showed highly significant statistical results ($P < 0.01$), while the control group showed extremely significant statistical results ($P < 0.001$), with the rate of change in the test group higher than that of the control group; at 28d, the test group showed extremely significant statistical results ($P < 0.001$), while the control group showed significant statistical results ($P < 0.01$), with the rate of change in the test group higher than that of the control group. At 7d, the control group had higher rates of change in R2, R5, R7, and F4 than the test group; at 14d, the test group had higher rates of change in R7 and F4 than the control group; at 28d, the test group had higher rates of change in R7 and F4 than the control group. At 7d, 14d, and 28d, the test group had higher rates of change than the control group. From the validation data, it can be concluded that at 7d, 14d, and 28d, there were no statistically significant differences between the test group and the control group in terms of moisture content, TEWL values, E values, elasticity measurements (R2, R5, R7), and firmness measurements (F4). This indicates that the two treatments had similar effects on improving sensitive skin.

PDRN (Polydeoxyribonucleotide) [5-6] and collagen [7] have significant application value in the field of anti-wrinkle treatments. PDRN activates the purinergic A2A receptor, which promotes collagen synthesis, improves skin elasticity, and reduces wrinkles. Additionally, PDRN has multiple functions, including anti-inflammatory effects, promotion of angiogenesis, and regulation of melanin production. Collagen, as the main structural protein of the skin, can directly enhance the skin's support and reduce the appearance of wrinkles when supplemented. Modifying PDRN and collagen into spherical structures enhances their transdermal absorption capabilities: Spherical nanoparticles or microparticles have a higher specific surface area and more uniform distribution characteristics, allowing for better contact with the skin and thus improving transdermal

absorption efficiency. This enables PDRN and collagen to more effectively penetrate the deeper layers of the skin and exert their anti-wrinkle effects. The spherical structure can reduce intermolecular interactions, lower the degradation rate, and thereby extend the duration of action of PDRN and collagen in the skin. Moreover, it reduces injection risks: Traditional injectable anti-wrinkle products may cause adverse reactions such as infection, allergy, and tissue damage. If the spherical PDRN and collagen complex can exert its effects through topical application, it will avoid the pain and potential risks associated with injections, providing a safer and more convenient option for those who are afraid of pain but seek aesthetic results. Developing a composite system of spherical PDRN and spherical collagen provides new ideas for anti-wrinkle efficacy: First, synergistic enhancement: PDRN and collagen have complementary mechanisms in anti-wrinkle effects. PDRN promotes collagen synthesis and skin regeneration, while collagen directly supplements the structural components of the skin. The combination of the two is expected to achieve synergistic enhancement and further improve anti-wrinkle effects. Second, multifunctional expansion: In addition to anti-wrinkle effects, PDRN also has anti-inflammatory and wound-healing properties. The spherical complex system can integrate these functions to develop multifunctional skincare products, such as those for acne scar repair and skin whitening. Finally, personalized application: The spherical complex system can achieve personalized anti-wrinkle effects by adjusting parameters such as particle size and concentration, meeting the needs of different skin types and demands. Despite the great potential of the spherical PDRN and spherical collagen composite system, further research is needed to verify its safety and efficacy. ** Future research directions may include: ① Clinical trials: Conducting large-scale, long-term clinical trials to evaluate the anti-wrinkle effects, safety, and synergistic effects with other skincare products of the spherical complex system. ② Mechanistic studies: Investigating the impact of the spherical structure on the biological activity of PDRN and collagen, as well as their mechanisms of action in the skin. ③ Product development: Developing product forms suitable for different application scenarios, such as serums, creams, and masks, to meet market demands. In summary, the composite system of spherical PDRN and spherical collagen provides new ideas and directions for the anti-wrinkle field, and is expected to offer safer and more effective choices for those pursuing aesthetic results.

3. Conclusion

Aiming at the dual skincare demands of repair and antiaging for sensitiveskin populations, this study constructed a PolyganTai® spherical PDRNspherical collagen composite system. By utilizing layered microsphere supramolecular assembly technology, the application bottlenecks of poor transdermal penetration and easy degradation of macromolecules, including PDRN and collagen, were alleviated. Confocal Raman spectroscopy verified that the spherical configuration markedly enhanced skin penetration performance of PDRN and collagen. Ex vivo skin model assays demonstrated that this composite system up-regulated the expression of eight collagen subtypes (Collagen I, III, IV, V, VI, VII, XVII, XVIII), elastin and collagen fibers, presenting remarkable antiwrinkle and skintightening bioactivities. Evaluations on the EpiKutis® 3D epidermal model revealed that the composite suppressed the secretion of inflammatory mediators IL1α, TNFα and PGE2. Meanwhile, it elevated filaggrin (FLG) and loricrin (LOR) levels and thickened viable epidermal layers, contributing to antiirritation and skinbarrier restoration. Splitface human clinical tests illustrated that this topical composite exhibited no statistically significant differences in moisturization, repair, antiwrinkle, tightening, and soothing effects compared with the salmonderived PDRN injection

group, with no adverse cutaneous reactions observed. In conclusion, the spherical PDRNspherical collagen composite acts as a topical antiaging candidate. It provides a safe and innovative strategy for antiaging and restoration of sensitive skin while avoiding potential risks associated with injection procedures.

Disclosure statement

The author declares no conflict of interest.

References

[1] Li L, 2010, Current Research Status of Sensitive Skin. Journal of Dermatology and Venereology, 2010(5): 5.

[2] Darvin ME, Fluhr JW, Caspers P, et al., 2009, In Vivo Distribution of Carotenoids in Different Anatomical Locations of Human Skin: Comparative Assessment with Two Different Raman Spectroscopy Methods. Experimental Dermatology, 18(12): 1060–1063.

[3] Franzen L, Selzer D, Fluhr JW, et al., 2013, Towards Drug Quantification in Human Skin with Confocal Raman Microscopy. European Journal of Pharmaceutics and Biopharmaceutics, 84(2): 437–444.

[4] Mickael M, Pudney PDA, Williamson AM, et al., 2009, Studying the Effectiveness of Penetration Enhancers to Deliver Retinol Through the Stratum Corneum by In Vivo Confocal Raman Spectroscopy. Journal of Controlled Release, 138(1): 32–39.

[5] Tian M, Sun L, Yan P, et al., 2024, Preparation of Polydeoxyribonucleotide (PDRN) Materials and Advances in Biomedical Research. Materials Science and Engineering, 32(4): 1–15.

[6] Hwang K-H, Kim J-H, et al., 2018, An Effective Range of Polydeoxyribonucleotides Is Critical for Wound Healing Quality. Molecular Medicine Reports, 18(6): 5166–5172.

[7] Extraction and Characterization of Type I Collagen from Parrotfish (Scarus sordidus Forsskål, 1775) Scale Solubilized with the Aid of Acetic Acid and Pepsin. 2023, International Journal of Biomaterials, 7312447.

Publisher's note

Bio-Byword Scientific Publishing remains neutral with regard to jurisdictional claims in published maps and institutional affiliations.